Frontiers in Neuroscience

Systemic inflammation differentially modulates the levels of EBI2 and CH25H/CYP7B1 enzymes in the brain microvascular cells

Fionä Caratis[1], Bartosz Karaszewski[2,3], Ilona Klejbor[4], Tomomi Furihata[5], Aleksandra Rutkowska[1,3*]

[1]Department of Anatomy and Neurobiology, Medical University of Gdansk, Gdansk, Poland
[2]Department of Adult Neurology, Medical University of Gdansk & University Clinical Center, Gdansk, Poland
[3]Brain Diseases Center, Medical University of Gdansk, Gdansk, Poland
[4]Department of Anatomy, Collegium Medicum, Jan Kochanowski University in Kielce, Kielce, Poland
[5]Laboratory of Clinical Pharmacy and Experimental Therapeutics, School of Pharmacy, Tokyo University of Pharmacy and Life Sciences, Hachioji, Tokyo, Japan

*Corresponding author:

Aleksandra Rutkowska
ola.rutkowska@gumed.edu.pl

KEYWORDS: neuroinflammation, oxysterols, EBI2, CH25H, CYP7B1, HSD3B7, blood-brain barrier, microvessels, pericytes, astrocytes, endothelial cells

ABSTRACT

The EBI2 receptor is a major modulator of innate immunity and, together with its ligand, oxysterol 7α,25OHC, has been implicated in several neuroinflammatory and autoimmune diseases. 7α,25OHC is synthesised from cholesterol with CH25H and CYP7B1 enzymes and degraded with HSD3B7. The concentration of 7α,25OHC in the brain increases in the early phases of the murine model of multiple sclerosis, leading to an enhanced central nervous system (CNS) infiltration with EBI2-expressing lymphocytes. Here, we aimed to investigate whether the enzymes involved in the synthesis and degradation of 7α,25OHC are expressed directly in the mouse brain microvascular cells and whether systemic inflammation modulates their levels in these cells. Normal mouse brain capillaries were isolated and immunostained for EBI2, CH25H, CYP7B1 and HSD3B7. Subsequently, mice were challenged with lipopolysaccharide and the mRNA expression in whole brain homogenates was measured. Changes in the receptor and enzyme levels were quantified directly in endothelial cells (ECs), pericytes and astrocytes. The data indicated high levels of EBI2 in the brain microvascular ECs, pericytes and astrocytes with the highest co-localisation in pericytes. CH25H was detected in ECs and astrocytes with low levels in pericytes. CYP7B1 was moderately expressed in ECs, astrocytes and pericytes. The 7α,25OHC degrading enzyme HSD3B7 was the least detected in astrocytes. Moreover, the data indicated that systemic inflammation downregulated the mRNA levels of *Ebi2* and upregulated *Ch25h* expression in the whole brain. Specifically in each cell type, EBI2 was not induced in ECs but increased in astrocytes and pericytes. CH25H levels increased in astrocytes and pericytes and CYP7B1 in ECs and astrocytes. The degrading enzyme, HSD3B7, was least affected by systemic inflammation. Taken together, we here demonstrate that EBI2 and the enzymes regulating its ligand levels are differentially expressed in mouse brain microvessels and are highly modulated by systemic inflammation. Upregulated concentration of 7α,25OHC in the brain during inflammation may lead to an increased migration of EBI2-expressing immune cells into the CNS during infection or neuroinflammatory disease. Modulation of the EBI2/oxysterol system in the brain or directly in the brain blood vessels may thus provide a new approach to treating neuroinflammatory diseases including multiple sclerosis.

INTRODUCTION

The GPR183 (also known as Epstein-Barr virus-induced gene 2 (EBI2)) is a G protein-coupled receptor discovered in 1993 in B lymphocytes (Birkenbach et al., 1993). Since then, EBI2 was shown to play important roles in the regulation of the innate and adaptive immune systems, cellular migration (Gatto et al., 2009; Hannedouche et al., 2011; Pereira et al., 2009; Preuss et al., 2014; Rutkowska et al., 2015; Rutkowska et al., 2016), inflammatory signalling (Clottu et al., 2017; Rutkowska et al., 2018; Wanke et al., 2017) and myelination in the central nervous system (CNS) (Nelissen et al., 2012; Rutkowska et al., 2017; Velasco-Estevez et al., 2021). Its most potent endogenous agonist is oxysterol 7α,25-dihydroxycholesterol (7α,25OHC) (Hannedouche et al., 2011; Liu et al., 2011). 7α,25OHC is synthesized from cholesterol by the sequential enzymatic activity of cholesterol 25-hydroxylase (CH25H) and 25-hydroxycholesterol 7-alpha-hydroxylase (CYP7B1) and metabolized by 3beta-hydroxy-Delta(5)-C27-steroid oxidoreductase (HSD3B7) (Russell, 2003) **(Figure 1A)**. 7α,25OHC was repeatedly shown to direct immune cell migration via an oxysterol gradient, both *in vivo* and *in vitro*, in EBI2-expressing cells demonstrating its key regulatory role in immune cell function and immunity (Clottu et al., 2017; Hannedouche et al., 2011; Liu et al., 2011; Preuss et al., 2014; Rutkowska et al., 2015; Rutkowska et al., 2016; Yi et al., 2012).

A challenge with bacterial lipopolysaccharide (LPS) induces the synthesis and release of oxysterols including the EBI2 ligand, 7α,25OHC. In one of the first studies looking at LPS and oxysterol levels, mouse macrophages challenged with LPS upregulated the CH25H enzyme 35-fold and increased 6- to 7-fold their cellular concentration of oxysterol 25OHC, the precursor to 7α,25OHC synthesised with the CH25H enzyme (Diczfalusy et al., 2009). We demonstrated that LPS-challenged primary mouse astrocytes synthesise and release oxysterols, including 7α,25OHC (Rutkowska et al., 2016). We also showed *in vitro* a rapid downregulation of the EBI2 transcripts upon LPS treatment and an increase in the mRNA levels of the CH25H and CYP7B1 enzymes in mouse astrocytes. Moreover, the levels of the EBI2 ligand 7α,25OHC were highly increased in the media from LPS-treated astrocytes indicating these cells as one of the sources of oxysterols in the brain during inflammation. Moreover, macrophages treated with media from LPS-treated astrocytes displayed increased migration, an effect inhibited with the EBI2 antagonist NIBR189, indicating EBI2/oxysterol-dependent mechanisms. Other groups demonstrated that primary human monocyte-derived macrophages challenged with LPS transiently increase expression of EBI2 and markedly upregulate the CH25H and CYP7B1 enzymes (Preuss et al., 2014). Similar upregulation of the CH25H and HSD3B7 enzymes was reported in LPS-treated BV2 microglia (Mutemberezi et al., 2018). Importantly, increased levels of 7α,25OHC were also found *in vivo* in the spleens and brains of LPS-challenged mice (Hannedouche et al., 2011; Liu et al., 2011; Mutemberezi et al., 2018) and this LPS-mediated effect was not detected in CH25H knock-out mice (Hannedouche et al., 2011).

In normal CNS, the entry of immune cells is limited by the blood-brain barrier (BBB), a physical barrier established at the level of the brain microvascular endothelial cells (ECs) by tight junction proteins and further supported and regulated by pericytes and astrocytic endfeet, among other cells (Armulik et al., 2010). The function of the barrier is compromised by a range of factors including inflammation, neurodegeneration, stroke and brain trauma, to name just a few. In multiple sclerosis (MS), a chronic inflammatory disease of the CNS, disruption of the BBB occurs focally and at very early stages facilitating the entry of peripherally activated lymphocytes into the brain parenchyma. Once in the brain, the lymphocytes trigger an inappropriate inflammatory response leading to the propagation of pro-inflammatory signalling and activation of local glial cells which leads to myelin damage and neuronal degeneration (Cramer et al., 2015; Spencer et al., 2018). In the animal model of MS, the experimental autoimmune encephalomyelitis (EAE), increased concentration of 7α,25OHC in mouse CNS was independently reported by two groups (Mutemberezi et al., 2018; Wanke et al., 2017). Wanke and colleagues (2017) established that the increase in 7α,25OHC levels resulted from the upregulation of CH25H by microglia and CYP7B1 by infiltrating lymphocytes during simultaneous downregulation of HSD3B7. Importantly, the increased concentration of the EBI2 ligand enhanced the migration of autoreactive T cells into the CNS during the early phases of transfer EAE, exacerbating the disease course. Similar conclusions were drawn in a study using the EAE model and CH25H knock-out mice

(Chalmin et al., 2015). The EAE severity was significantly attenuated in the CH25H deficient mice in part by reduced trafficking of encephalitogenic CD4+ T cells into the CNS. The levels of oxysterols in the plasma and the cerebrospinal fluid (CSF) also change dynamically in humans in the course of inflammatory diseases. Crick and colleagues (2017) measured a wide range of oxysterols in the CSF and plasma of patients diagnosed with relapsing-remitting MS, clinically isolated syndrome (CIS), neurodegenerative diseases including Parkinson's and Alzheimer's disease, amyotrophic lateral sclerosis and other inflammatory CNS diseases. Specifically in MS patients, the levels of 25OHC, the precursor to 7α,25OHC, were reduced in the plasma and increased only in the CSF in relapsing-remitting MS indicating disease-specific modulation of oxysterol levels in the CNS.

In mice deficient in the CH25H enzyme, activated B cells fail to migrate to the outer- and inter-follicular regions of the T cell follicles and favour the B-T cell boundary and the central areas of the follicles (Hannedouche et al., 2011). These CH25H-deficient mice also show a three-fold decrease in the extent of their antibody response. In contrast, saturating the follicular microenvironment with 7α,25OHC or inhibition of the second enzyme, CYP7B1, results in equal distribution of B cells in the lymphoid tissue suggesting that the 7α,25OHC gradient is crucial for appropriate localization of B cells in the lymphoid tissue (Hannedouche et al., 2011; Liu et al., 2011). Thus, to ensure a correct humoral antibody response, the gradient of 7α,25OHC is tightly controlled. Since B cells do not themselves express the 7α,25OHC synthesising (CH25H and CYP7B1) nor the degrading enzyme (HSD3B7) they depend on other cells to regulate the gradient. Indeed, it has been shown that lymphoid stromal cells upregulate the levels of 7α,25OHC via CH25H and CYP7B1 enzymes and follicular dendritic cells downregulate its levels via the HSD3B7 enzyme (Yi et al., 2012).

Here, we aimed to identify whether EBI2 and the enzymes in the 7α,25OHC synthetic pathway (CH25H, CYP7B1, HSD3B7) are differentially expressed in the brain microvascular cells and whether systemic inflammation modulates their levels specifically in these cells. Regulation of 7α,25OHC levels by the brain microvascular cells may help in the identification of novel drug targets for the modulation of neuroinflammatory signalling and immune cell trafficking into the CNS.

MATERIALS AND METHODS

Animals

All animal experiments were approved by the Local Ethical Committee for Animal Experiments in Bydgoszcz, Poland under licence numbers 27/2019 and 38/2021. The C57BL/6 male mice were housed in standard cages with an enriched environment under 12-hour day and night cycles. The air in the room was exchanged 15 times per hour, the temperature was kept at 20-23ºC and the humidity was between 50-60%. The animals had unrestricted access to food and water.

LPS *in vivo* model

Forty-eight three-month-old male C57BL/6 mice were used. The mice received intraperitoneal (i.p.) injections of 0,9% NaCl (vehicle) or 2 mg/kg LPS for 12 or 24 hours (h). The mice were anaesthetised with isoflurane and perfused with NaCl for subsequent biochemical analysis or 2% paraformaldehyde (PFA) for immunohistochemistry. Whole brains were removed, snap-frozen and stored at -80°C for subsequent biochemical analysis or put into the O.C.T. compound and cut into 40 µm sections with a cryostat. The cut slices were submerged in anti-freeze and stored at -20ºC until used for immunohistochemistry. The snap-frozen brains (right hemispheres) were homogenised with a pestle and a mortar in liquid nitrogen. The resulting powder was then suspended in 400 µL of fenozol/50 mg of tissue and frozen at -80°C until needed. The left hemispheres were homogenised with a Dounce homogeniser in RIPA buffer supplemented with a protein inhibitor cocktail (700 µl/100 mg of tissue) and centrifuged at 13.4k rpm for 20 minutes at 4°C. The supernatant was then aliquoted for ELISAs and stored at -80°C until needed.

Mouse microvessel isolation

Postnatal day 10 (P10) C57BL/6 mice were used for brain microvessel isolation according to the protocols by Paraiso et al. and Hartz et al. (Hartz et al., 2018; Paraiso et al., 2020). Briefly, the brain was extracted from the skull, the cerebral cortex was separated from the rest of the brain and the

meninges were removed. Cortices were placed in the isolation buffer: 5 mM glutaMAX and 1 mM sodium pyruvate in DPBS with calcium and magnesium, pH 7.4 at 4ºC. Cortices were then homogenised in the isolation buffer with a Dounce homogeniser for 20 strokes. The homogenate was moved to 2 ml tubes and then 40% polysucrose 400 (P7798-100 g, Merck) in DPBS with calcium and magnesium was added in equal volumes for a final concentration of 20%. After vigorous shaking, the homogenates were centrifuged at 7.7k rpm for 15-20 minutes at 4°C (fixed angle rotor). The pellet was resuspended in 1% bovine serum albumin (BSA) in the isolation buffer and was then filtered through a 300 µm mesh. The mesh was washed with 4 ml of the BSA-containing isolation buffer. The flow-through was filtered through a 30 µm cell strainer twice and the mesh was washed twice with BSA-containing isolation buffer before discarding the filtrate. The filter was turned upside-down and washed twice with BSA-isolation buffer to wash off the capillaries. After collection, the capillaries were centrifuged at 1500 rpm for 3 minutes at 4°C and resuspended in the isolation buffer. The capillaries were centrifuged and resuspended in the isolation buffer for subsequent analysis. The capillaries were left to adhere to the bottom of the plate in the isolation buffer in the incubator at 37°C and 5% CO_2.

Real-time quantitative polymerase chain reaction (RT-qPCR)

RNA was isolated using the total RNA mini plus kit (036-100, AA Biotech, Poland) according to the manufacturer's protocol. The cDNA synthesis was performed with a transcriba kit (4000, AA Biotech, Poland) using the following programme: 60 minutes at 42°C followed by 5 minutes at 70°C or using the high-capacity cDNA reverse transcription kit (4368814, ThermoFisher) with the following programme: 10 minutes at 25°C followed by 120 minutes at 37°C and 5 seconds at 85°C. The RT-qPCR was then performed with the TaqMan fast advanced master mix (4444557, ThermoFisher) or the Sensitive RT HS-PCR Mix (2017-2000, AA Biotech, Gdansk, Poland) on the LightCycler480 (Roche) according to the manufacturer's protocol. All samples were run in duplicate. The following FAM dye-labelled Taqman (Applied Biosystems) primers were used: β-actin (Mm02619580_g1), GAPDH (Mm99999915_g1), EBI2 (Mm02620906_s1), CH25H (Mm00515486_s1), CYP7B1 Mm00484157_m1), HSD3B7 (Mm01159156_g1), Occludin (Mm00500912_m1), N-cadherin (Mm01162490_m1). The relative gene expression was determined after normalisation to the housekeeping gene using the ΔCt (baseline gene expression in normal tissue) or ΔΔCt for comparisons of gene expression between treated and untreated samples.

Immunohistochemistry of mouse brain sections

The mouse sections in anti-freeze were washed in PBS for 3 x 5 minutes and then incubated in cold 4% PFA for 5 minutes at room temperature (RT) followed by incubation in 20% ice-cold methanol for 1 minute. The sections were then washed for 3 x 5 minutes with PBS and blocked for 6 hours at RT with PBS supplemented with 10% BSA, 0.5% Triton-X and 1% normal goat serum (NGS). Blocked sections were incubated overnight at RT with primary antibodies diluted in the following solution: PBS supplemented with 2% BSA and 0.1% Triton-X. Primary antibodies (1:100 unless stated otherwise) used were: goat anti-EBI2 (RRID: AB_1090369, ab121001, Abcam), rabbit polyclonal CH25H (600-401-MM8, ThermoFisher), mouse monoclonal CYP7B1 (OTI1G7) (TA807549, ThermoFisher), rabbit polyclonal HSD3B7 (RRID: AB_10856786, BS-2366R, ThermoFisher), mouse monoclonal Iba1 (GT10312) (1:200) (RRID: AB_2735228, MA5-27726, ThermoFisher), rabbit Iba1 (RRID:AB_839504, 019-19741, Wako), mouse monoclonal GFAP antibody (1:200) (RRID: AB_2827276, SAB5201104, Sigma-Aldrich), rabbit monoclonal GFAP (1:200) (RRID: AB_2631098, 12389, CellSignalling), mouse monoclonal CD31 (PECAM-1) (RRID: AB_10596359, BMS137, eBioscience), rabbit polyclonal CD31 (PECAM-1) (RRID: AB_10981955, PA5-16301, ThermoFisher), rabbit monoclonal PDGFRβ (RRID: AB_10985851, MA5-15143, ThermoFisher), goat polyclonal PDGFRb (RRID: AB_2162633, AF1042, R&D Systems), rabbit polyclonal occludin (RRID: AB_2533468, 40-4700, ThermoFisher), mouse monoclonal N-cadherin (3B9) (RRID: AB_2313779, 333900, ThermoFisher). The following day, sections were washed 3 x 10 minutes in PBS and incubated for 2 hours at RT with the following secondary antibodies (1:500): goat anti-mouse IgG (H+L) cross-adsorbed Alexa Fluor 546 (RRID: AB_2534071, A-11003, ThermoFisher), goat anti-mouse IgG (H+L) cross-adsorbed Alexa Fluor 488 (RRID: AB_2338840, 115-545-003-20, JacksonImmuno), goat anti-rabbit IgG (H+L) cross-adsorbed Alexa Fluor 488 (RRID: AB_2630356, ab150077, abcam), donkey anti-goat IgG (H+L) cross-adsorbed Alexa Fluor 546 (RRID: AB_2534103, A11056, ThermoFisher)and

Hoechst33342 (H1399, ThermoFisher). The sections were then washed 3 x 10 minutes in PBS, air-dried, mounted with Keiser's gelatine and imaged using a confocal Zeiss LSM880 microscope.

Immunohistochemistry of isolated brain microvessels

After isolation, mouse capillaries were plated in PBS on poly-D-lysine coated 8-well µ-slide plates (80826, Ibidi) and left to adhere for 2 hours in the incubator at 37°C and 5% CO_2. The media was removed and the capillaries were left to air dry for 30 minutes. The capillaries were washed once in PBS and then fixed in 4% PFA for 10 minutes. The PFA was removed and 50 µl of ice-cold methanol was added for 1 minute. The capillaries were then washed twice with PBS at RT and blocked for 1 hour in 0.5% NGS, 1% BSA and 0.1% Tween20 in PBS. Subsequently, the capillaries were incubated overnight at 4°C in 0.5% BSA and 0.05% Tween20 in PBS with the primary antibodies. Primary antibodies used for mouse microvessels (1:100) were: goat polyclonal EBI2 (RRID: AB_10903697, ab121001, Abcam), rabbit polyclonal CH25H (600-401-MM8, ThermoFisher), mouse monoclonal CYP7B1 (OTI1G7) (TA807549, ThermoFisher), rabbit polyclonal HSD3B7 (RRID: AB_10856786, BS-2366R, ThermoFisher), rabbit monoclonal GFAP (RRID: AB_2631098, 12389, CellSignalling), mouse monoclonal GFAP antibody (1:200) (RRID: AB_2827276, SAB5201104, Sigma-Aldrich), mouse monoclonal CD31 (PECAM-1) (RRID: AB_10596359, BMS137, eBioscience), rabbit polyclonal CD31 (PECAM-1) (RRID: AB_10981955, PA5-16301, ThermoFisher), goat polyclonal PDGFRβ (RRID: AB_2162633, AF1042, R&D Systems), rabbit monoclonal PDGFRβ (RRID: AB_10985851, MA5-15143, ThermoFisher). The capillaries were washed twice with PBS, once in 0.5% BSA with 0.05% Tween20 in PBS for 10 minutes and incubated with secondary antibodies and Hoechst33342 (H1399, ThermoFisher) for 1 hour at RT in the dark. The following secondary antibodies were used: goat anti-mouse IgG (H+L) cross-adsorbed Alexa Fluor 546 (RRID: AB_2534071, A-11003, ThermoFisher), goat anti-mouse IgG (H+L) cross-adsorbed Alexa Fluor 488 (RRID: AB_2338840, 115-545-003-20, JacksonImmuno), goat anti-rabbit IgG (H+L) cross-adsorbed Alexa Fluor 488 (RRID: AB_2630356, ab150077, abcam), donkey anti-goat IgG (H+L) cross-adsorbed Alexa Fluor 546 (RRID: AB_2534103, A11056, ThermoFisher)and Hoechst33342 (H1399, ThermoFisher). The capillaries were then washed three times in PBS and once in ddH_2O for 10 minutes, air-dried, mounted with Keiser's gelatine and imaged with Zeiss LSM880 confocal microscope.

Enzyme-linked immunosorbent assay (ELISA)

ELISAs were performed using DuoSet ELISA kits: mouse IL-6 (DY406-05), mouse IL-1b/1F2 (DY401-05) and mouse TNF-α (DY410-05) from R&D Systems according to the manufacturer's instructions. Briefly, 100 µl of samples or standards in reagent diluent, 1% BSA in PBS, were added to a 96-well plate and incubated for 2 hours at RT. The wells were then emptied and washed three times with the wash buffer, 0.05% Tween-20 in PBS. Subsequently, 100 µl of the detection antibody diluted in the supplied reagent diluent was added to each well for 2 hours at RT. The plate was washed again with the wash buffer and 100 µl of streptavidin-HRP was added to each well for 20 minutes at RT in the dark. The plate was again washed three times and 100 µl of the substrate solution, 1:1 H_2O_2 and tetramethyl benzidine (34021, LifeTechnologies), was added to each well for 20 minutes at RT. To stop the reaction, 50 µl of H_2SO_4 1 mol/L, was added to the wells and mixed gently. Optical density was read at 450 nm with a VICTOR Nivo plate reader (PerkinElmer).

Statistical analysis

All statistical analysis was performed with GraphPad Prism 9 applying unpaired student t-tests for comparisons of two groups. Data are shown as mean +/- standard error of the mean (SEM). Where appropriate, p values are written in the figure legends with significant effects indicated by asterisks: *$p<0.05$, **$p<0.01$, ***$p<0.001$, ****$p<0.0001$. Grubbs' tests were run to identify and remove outliers.

RESULTS

The oxysterol 7α,25OHC synthesising (CH25H, CYP7B1) and degrading (HSD3B7) enzymes are present in the mouse brain microvascular cells.

It was demonstrated before that primary mouse astrocytes and BV2 microglia regulate oxysterol levels *in vitro* and *in vivo* under normal and inflammatory conditions but the expression of EBI2 and the 7α,25OHC synthesising (CH25H, CYP7B1) and degrading (HSD3B7) enzymes directly in the brain microvascular cells has not been investigated (Mutemberezi et al., 2018; Rutkowska et al., 2016). For

261 this purpose, we isolated normal mouse brain microvessels and quantified the receptor and enzyme
262 levels. The data showed that the EBI2 receptor and the three enzymes were differentially present in the
263 isolated normal mouse brain microvessels. EBI2 highly co-localised with pericytes/smooth muscle cells
264 (PGFRβ+ cells) and the ECs (CD31+ cells) and to a lesser degree with astrocytic endfeet (GFAP+)
265 **(Figure 1B)**. The CH25H enzyme highly co-localised with CD31+ (ECs) and GFAP+ cells (astrocytic
266 endfeet) and very lightly with PDGFRβ+ cells (pericytes/smooth muscle cells) **(Figure 1C)**. The second
267 enzyme in the 7α,25OHC synthetic pathway, CYP7B1, was moderately and to a similar degree present
268 in CD31+ (ECs), GFAP+ (astrocytic endfeet) and PDGFRβ+ cells (pericytes/smooth muscle cells)
269 **(Figure 1D)**. The 7α,25OHC degrading enzyme HSD3B7 was highly present in CD31+ (ECs) and
270 PDGFRβ+ cells (pericytes/smooth muscle cells) and at very low levels in GFAP+ cells (astrocytic
271 endfeet) **(Figure 1E)**.

272 **Systemic inflammation induces changes in the expression of *Ebi2* and *Ch25H*, *Cyp7b1* and *Hsd3b7***
273 **enzymes in the mouse brain.**
274 Peripheral injections of LPS were shown previously to induce neuroinflammation and disruption of the
275 BBB (Banks et al., 2015; Li et al., 2020). We also demonstrated that repeated peripheral injections with
276 LPS induce a significant increase in the number of pro-inflammatory cytokines in the mouse brain
277 (Rutkowska et al., 2018). The disruption of the BBB function and the extent of neuroinflammation
278 depend heavily on the applied protocol, particularly on the dose and frequency of LPS injections (Wang
279 et al., 2014). Here, the applied protocol of a single high dose (2 mg/kg) intraperitoneal (i.p.) LPS
280 injection induced astrocyte and microglia activation in the hippocampal region and pro-inflammatory
281 cytokine release in the mouse brain after 12 (IL6 and IL1β) and 24 hours (IL1β) **(Supplemental Figure**
282 **1)**. The mRNA levels of *occludin* and *N-cadherin* were downregulated after 12 and 24 hours of LPS
283 treatment **(Supplemental Figure 2)**. On the whole, the data indicates that the applied protocol induces
284 neuroinflammation and affects the expression of *occludin* and *N-cadherin*.

285 In the EAE model, the concentration of the 7α,25OHC ligand in the CNS is sharply elevated as a result
286 of the enhanced release of 7α,25OHC-synthesising enzymes, CH25H and CYP7B1, leading to an
287 increased brain infiltration by peripheral immune cells (Mutemberezi et al., 2018; Wanke et al., 2017).
288 Here, using the single high-dose LPS model, we investigated whether the EBI2/7α,25OHC system is
289 affected in the brain during acute systemic inflammation **(Figure 2A)**. The *Ebi2* transcripts in whole
290 brain homogenates were downregulated after 12 and 24 hours of LPS injection **(Figure 2B)**. The first
291 7α,25OHC synthesising enzyme, *Ch25h*, was strongly upregulated at both time points **(Figure 2C)** and
292 *Cyp7b1* decreased 12 hours after the LPS challenge and then levelled with the vehicle-treated after 24
293 hours **(Figure 2D)**. The mRNA levels of the degrading enzyme, *Hsd3b7*, slowly increased after LPS
294 treatment with significant changes observed after 24 hours **(Figure 2E)**.

295 **Systemic inflammation induces 7α,25OHC synthesising enzymes in the mouse brain vascular cells.**
296 After establishing that acute systemic inflammation modulates the expression of the EBI2/oxysterol
297 system at the whole-brain level, we then set out to determine whether the specific vascular cells were
298 also contributing. The increase in co-localisation of proteins after normalisation to the vehicle was
299 quantified in immunohistochemically stained brain sections. The data indicated an increase in the
300 number of co-localising pixels in EBI2+/GFAP+ and EBI2+/PDGFRβ+ cells and no increase in
301 EBI2+/CD31+ cells indicating that ECs in contrast to astrocytes and pericytes/smooth muscle cells do
302 not increase their baseline expression of EBI2 during acute peripheral inflammation **(Figure 3A)**. The
303 increase in CH25H enzyme co-localisation was observed for GFAP+ and PDGFRβ+ cells with only low
304 increase in CD31+ cells indicating that astrocytic endfeet and pericytes/smooth muscle cells are
305 regulating the levels of CH25H in the mouse brain vessels during acute inflammation **(Figure 3B)**. The
306 co-localisation of the CYP7B1 enzyme did not increase above the vehicle-treated levels in PDGFRβ+
307 cells but highly increased in CD31+ cells and moderately in GFAP+ cells **(Figure 3C)**. The 7α,25OHC
308 degrading enzyme, HSD3B7, was the least affected by LPS treatment with only a slight increase in co-
309 localisation in CD31+, GFAP+ and PDGFRβ+ cells **(Figure 3D)**.

310 **DISCUSSION**

311 The expression of EBI2 and CH25H, CYP7B1 and HSD3B7 enzymes in cells and tissue is dynamically
312 regulated especially under inflammatory conditions and is dependent on several factors i. the disease

313 and the animal model, ii. the applied *in vitro* or *in vivo* protocol, iii. the cell type, and iv. species, to
314 name just a few (Chalmin et al., 2015; Crick et al., 2017; Mutemberezi et al., 2018; Preuss et al., 2014;
315 Rutkowska et al., 2016; Wanke et al., 2017). Identification of the cellular source of oxysterols in the
316 brain, the magnitude and type of response (up- versus down-regulation), as well as the specificity of the
317 cellular response to a given inflammatory factor, may help in the discovery of new drug targets for the
318 modulation of immune cell trafficking into the CNS during systemic infection, neuroinflammatory or
319 neurodegenerative diseases. Here, we first aimed to determine if the EBI2 receptor and CH25H,
320 CYP7B1 and HSD3B7 enzymes are present in normal mouse brain microvessels. We established that
321 EBI2 is highly present in ECs, pericytes/smooth muscle cells and astrocytic endfeet. The three enzymes
322 were also detected to a variable degree in each cell type indicating that the microvascular cells contribute
323 to the synthesis, and possibly gradient formation and maintenance, of oxysterol 7α,25OHC in the brain
324 vasculature under normal conditions. The second aim of this study was to determine if EBI2, CH25H,
325 CYP7B1 and HSD3B7 are modulated in the brain vasculature under inflammatory conditions. Indeed,
326 EBI2 and the 7α,25OHC synthesising enzymes, CH25H and CYP7B1, were highly modulated in the
327 brain vasculature during acute inflammation. Again, the degree of modulation differed depending on the
328 enzyme and cell type indicating a specific microenvironment where levels of oxysterols are locally
329 modulated and controlled. Such tightly controlled oxysterol microenvironment is also established and
330 maintained in T cell follicles by differential CH25H, CYP7B1 and HSD3B7 enzyme expression by
331 lymphoid stromal cells and follicular dendritic cells which locally increase or decrease 7α,25OHC
332 levels, respectively (Yi et al., 2012). The established and maintained 7α,25OHC gradient is crucial for
333 the appropriate localization of B cells in the lymphoid tissue and the launching of an immune response.

334 The concentration of 7α,25OHC in the mouse CNS increases in the EAE model of MS (Mutemberezi et
335 al., 2018; Wanke et al., 2017). Again, the increase in 7α,25OHC levels results from differential
336 regulation of CH25H, CYP7B1 and HSD3B7 enzymes by different cells including microglia and
337 infiltrating lymphocytes (Wanke et al., 2017). The subsequent increase in the concentration of the EBI2
338 ligand, 7α,25OHC, enhances the migration of autoreactive T cells into the CNS and exacerbates the
339 disease course. Similar results were obtained in the EAE model performed in CH25H knock-out mice
340 where the disease severity was significantly attenuated as a result of reduced trafficking of memory
341 CD4+ T cells into the CNS (Chalmin et al., 2015). Natalizumab, a disease-modifying therapy for MS,
342 is a humanized IgG4 antibody against the α4-integrin subunit, which works by blocking the interaction
343 between the α4 integrin expressed on lymphocytes and VCAM1 expressed on ECs thus limiting the
344 passage of autoreactive lymphocytes across the vessel walls into the CNS (Brummer et al., 2021).
345 Modulation of the levels of CH25H, CYP7B1 and HSD3B7 enzymes directly in the microvasculature
346 may be another way to limit the entry of EBI2-expressing encephalitogenic immune cells into the CNS
347 during acute inflammation, neuroinflammatory disease or neurodegenerative diseases.

348 At the whole brain level, we reported downregulation of *Ebi2* transcripts after the LPS challenge while
349 the EBI2 protein analysis indicated an increase of EBI2 in GFAP+ and PDFGRβ+ cells. What may seem
350 an inconsistency is most likely due to a wider and diverse cellular content in hole brain homogenates
351 and different dynamics of EBI2 expression in various cells in response to inflammatory signalling.
352 Indeed, different dynamics of EBI2 expression were reported before. For instance, we found a decrease
353 in *Ebi2* mRNA levels in LPS-treated primary mouse astrocytes (Rutkowska et al., 2016), while others
354 reported a temporary increase in *EBI2* expression in primary human macrophages after LPS challenge
355 (Preuss et al., 2014). Here, we also observed major differences in EBI2 density between the ECs,
356 astrocytic endfeet and pericytes/smooth muscle cells. For instance, the ECs (CD31+ cells) and microglia
357 (Iba1+ cells) **(Supplemental Figure 3A)** did not increase EBI2 after LPS challenge (the quantification
358 method applied does not allow to measure downregulation and is represented here as no increase) while
359 GFAP+ and PDGFRβ+ cells increased. Taken together, the combined *Ebi2* transcripts from all cell types
360 present in the brain may indicate downregulation after LPS challenge while at the same time, specific
361 cells may upregulate *Ebi2*. As a side note, endogenous downregulation of EBI2 during mycobacterium
362 tuberculosis infection in macrophages was shown to contain early bacterial infection and intracellular
363 survival (Tang et al., 2020). The downregulated *Ebi2* expression in the whole brain after LPS challenge
364 reported here may indicate a protective mechanism during bacterial infection (LPS challenge) in the
365 CNS involving the EBI2 receptor.

Similarly, the expression of *Cyp7b1* initially decreased 12 hours after LPS treatment and started to return to baseline after 24 hours at the whole brain level. Whether the mRNA levels of *Cyp7b1* continued rising after 24 hours of LPS treatment remains to be elucidated, however, analysis of the protein levels, specifically in the brain microvascular cells indicated increased levels of CYP7B1 after LPS treatment in ECs and astrocytic endfeet and no induction in pericytes/smooth muscle cells (PDGFRβ+ cells). In a previous study of ours, we reported maximal mRNA expression of *Cyp7b1* after 24 hours of *in vitro* treatment with LPS while the levels of oxysterols 25OHC and 7α,25OHC peaked already after 15 hours indicating different dynamics of mRNA levels and oxysterol synthesis (Rutkowska et al., 2016). Moreover, Mutemberezi and colleagues (2018) demonstrated that the LPS challenge induces 7α,25OHC levels in the mouse brain after as little as 4 hours and declines thereafter.

Lastly, the 7α,25OHC degrading enzyme, HSD3B7, was strongly expressed in all three brain vascular cell types here studied and was least affected by inflammatory signalling. It is possible that during inflammation, the 7α,25OHC-synthesising enzymes, CH25H and CYP7B1, may be upregulated and the degrading enzyme, HSD3B7, may remain constant or be downregulated thus allowing for an increase in the concentration of 7α,25OHC in the inflamed tissue and a subsequent increase in immune cell infiltration of the inflamed tissue.

Taken together, these data indicate that the enzymes regulating the levels of 7α,25OHC are released directly by the brain microvascular cells. Moreover, the levels of EBI2 and CH25H, CYP7B1 are heavily regulated in the brain and the brain blood vascular cells during acute peripherally-induced inflammation. Modulation of EBI2 signalling and/or local concentrations of CH25H, CYP7B1 and HSD3B7 in the brain blood vessels might result in disease-modulatory effects with potential therapeutic applications in the treatment of neuroinflammatory diseases including multiple sclerosis.

LIST OF ABBREVIATIONS

BBB – blood-brain barrier
CNS – central nervous system
EAE – experimental autoimmune encephalomyelitis
EBI2 – Epstein-Barr virus-induced gene 2
EC – Endothelial cell
LPS – lipopolysaccharide
MS – multiple sclerosis

DECLARATIONS

Ethics approval and consent to participate

All animal experiments were approved by the Local Ethical Committee for Animal Experiments in Bydgoszcz, Poland under licence numbers 27/2019 and 38/2021.

Availability of data and materials

The data is available from the corresponding author upon reasonable request.

Competing interests

The authors declare that they have no competing interests

Funding

This project received funding from the National Science Centre, Poland, grant registration number: 2019/33/B/NZ4/03000 (AR).

Author's contributions

A.R. conceptualised the study, acquired funding, supervised the study and did the visualisation. B.K. and A.R. are responsible for the project administration and coordination. F.C. and A.R. designed the methodology, performed the investigations, data analysis and wrote the original draft. I.K. performed

the mouse *in vivo* model. B.K and T.F. reviewed and edited the manuscript. All authors accepted the final version of the manuscript.

Acknowledgements
We would like to thank Ms Beata Muszyńska from the Tricity Academic Experimental Animal House for her support with the *in vivo* mouse model.

REFERENCES

Armulik, A., Genové, G., Mäe, M., Nisancioglu, M.H., Wallgard, E., Niaudet, C., He, L., Norlin, J., Lindblom, P., Strittmatter, K., Johansson, B.R., Betsholtz, C., 2010. Pericytes regulate the blood–brain barrier. Nat. 2010 4687323 468, 557–561. https://doi.org/10.1038/nature09522

Banks, W.A., Gray, A.M., Erickson, M.A., Salameh, T.S., Damodarasamy, M., Sheibani, N., Meabon, J.S., Wing, E.E., Morofuji, Y., Cook, D.G., Reed, M.J., 2015. Lipopolysaccharide-induced blood-brain barrier disruption: roles of cyclooxygenase, oxidative stress, neuroinflammation, and elements of the neurovascular unit. J. Neuroinflammation 12. https://doi.org/10.1186/S12974-015-0434-1

Birkenbach, M., Josefsen, K., Yalamanchili, R., Lenoir, G., Kieff, E., 1993. Epstein-Barr virus-induced genes: first lymphocyte-specific G protein-coupled peptide receptors. J. Virol. 67, 2209–2220.

Brummer, T., Ruck, T., Meuth, S.G., Zipp, F., Bittner, S., 2021. Treatment approaches to patients with multiple sclerosis and coexisting autoimmune disorders. Ther. Adv. Neurol. Disord. 14. https://doi.org/10.1177/17562864211035542

Chalmin, F., Rochemont, V., Lippens, C., Clottu, A., Sailer, A.W.W., Merkler, D., Hugues, S., Pot, C., 2015. Oxysterols regulate encephalitogenic CD4+ T cell trafficking during central nervous system autoimmunity. J. Autoimmun. 56, 45–55. https://doi.org/10.1016/j.jaut.2014.10.001

Clottu, A.S., Mathias, A., Sailer, A.W., Schluep, M., Seebach, J.D., Du Pasquier, R., Pot, C., 2017. EBI2 Expression and Function: Robust in Memory Lymphocytes and Increased by Natalizumab in Multiple Sclerosis. Cell Rep. 18, 213–224. https://doi.org/10.1016/j.celrep.2016.12.006

Cramer, S.P., Modvig, S., Simonsen, H.J., Frederiksen, J.L., Larsson, H.B.W., 2015. Permeability of the blood-brain barrier predicts conversion from optic neuritis to multiple sclerosis. Brain 138, 2571–83. https://doi.org/10.1093/brain/awv203

Crick, P.J., Griffiths, W.J., Zhang, J., Beibel, M., Abdel-Khalik, J., Kuhle, J., Sailer, A.W., Wang, Y., 2017. Reduced Plasma Levels of 25-Hydroxycholesterol and Increased Cerebrospinal Fluid Levels of Bile Acid Precursors in Multiple Sclerosis Patients. Mol. Neurobiol. 54, 8009–8020. https://doi.org/10.1007/s12035-016-0281-9

Diczfalusy, U., Olofsson, K.E., Carlsson, A.M., Gong, M., Golenbock, D.T., Rooyackers, O., Fläring, U., Björkbacka, H., 2009. Marked upregulation of cholesterol 25-hydroxylase expression by lipopolysaccharide. J. Lipid Res. 50, 2258–2264. https://doi.org/10.1194/JLR.M900107-JLR200

Gatto, D., Paus, D., Basten, A., Mackay, C.R., Brink, R., 2009. Guidance of B Cells by the Orphan G Protein-Coupled Receptor EBI2 Shapes Humoral Immune Responses. Immunity 31, 259–269. https://doi.org/10.1016/j.immuni.2009.06.016

Hannedouche, S., Zhang, J., Yi, T., Shen, W., Nguyen, D., Pereira, J.P., Guerini, D., Baumgarten, B.U., Roggo, S., Wen, B., Knochenmuss, R., Noël, S., Gessier, F., Kelly, L.M., Vanek, M., Laurent, S., Preuss, I., Miault, C., Christen, I., Karuna, R., Li, W., Koo, D.-I.I., Suply, T., Schmedt, C., Peters, E.C., Falchetto, R., Katopodis, A., Spanka, C., Roy, M.-O.O., Detheux, M., Chen, Y.A., Schultz, P.G., Cho, C.Y., Seuwen, K., Cyster, J.G., Sailer, A.W., 2011. Oxysterols direct immune cell migration via EBI2. Nature 475, 524–527. https://doi.org/10.1038/nature10280

459 Hartz, A.M.S., Schulz, J.A., Sokola, B.S., Edelmann, S.E., Shen, A.N., Rempe, R.G., Zhong, Y.,
460 Seblani, N. El, Bauer, B., 2018. Isolation of Cerebral Capillaries from Fresh Human Brain
461 Tissue. J. Vis. Exp. 2018. https://doi.org/10.3791/57346

462 Li, T., Zheng, L.N., Han, X.H., 2020. Fenretinide attenuates lipopolysaccharide (LPS)-induced blood-
463 brain barrier (BBB) and depressive-like behavior in mice by targeting Nrf-2 signaling. Biomed.
464 Pharmacother. 125, 109680. https://doi.org/10.1016/J.BIOPHA.2019.109680

465 Liu, C., Yang, X. V., Wu, J., Kuei, C., Mani, N.S., Zhang, L., Yu, J., Sutton, S.W., Qin, N., Banie, H.,
466 Karlsson, L., Sun, S., Lovenberg, T.W., 2011. Oxysterols direct B-cell migration through EBI2.
467 Nature 475, 519–523. https://doi.org/10.1038/nature10226

468 Mutemberezi, V., Buisseret, B., Masquelier, J., Guillemot-Legris, O., Alhouayek, M., Muccioli, G.G.,
469 2018. Oxysterol levels and metabolism in the course of neuroinflammation: insights from in vitro
470 and in vivo models. J. Neuroinflammation 15, 74. https://doi.org/10.1186/s12974-018-1114-8

471 Nelissen, K., Mulder, M., Smets, I., Timmermans, S., Smeets, K., Ameloot, M., Hendriks, J.J.A.,
472 2012. Liver X receptors regulate cholesterol homeostasis in oligodendrocytes. J. Neurosci. Res.
473 90, 60–71. https://doi.org/10.1002/jnr.22743

474 Paraiso, H.C., Wang, X., Kuo, P.C., Furnas, D., Scofield, B.A., Chang, F.L., Yen, J.H., Yu, I.C., 2020.
475 Isolation of Mouse Cerebral Microvasculature for Molecular and Single-Cell Analysis. Front.
476 Cell. Neurosci. 14. https://doi.org/10.3389/FNCEL.2020.00084/PDF

477 Pereira, J.P., Kelly, L.M., Xu, Y., Cyster, J.G., 2009. EBI2 mediates B cell segregation between the
478 outer and centre follicle. Nature 460, 1122–1126. https://doi.org/10.1038/nature08226

479 Preuss, I., Ludwig, M.-G.G., Baumgarten, B., Bassilana, F., Gessier, F., Seuwen, K., Sailer, A.W.,
480 2014. Transcriptional regulation and functional characterization of the oxysterol/EBI2 system in
481 primary human macrophages. Biochem. Biophys. Res. Commun. 446, 663–668.
482 https://doi.org/10.1016/j.bbrc.2014.01.069

483 Russell, D.W., 2003. The enzymes, regulation, and genetics of bile acid synthesis. Annu. Rev.
484 Biochem. 72, 137–174. https://doi.org/10.1146/ANNUREV.BIOCHEM.72.121801.161712

485 Rutkowska, A., O'Sullivan, S.A., Christen, I., Zhang, J., Sailer, A.W., Dev, K.K., 2016. The EBI2
486 signalling pathway plays a role in cellular crosstalk between astrocytes and macrophages. Sci.
487 Rep. 6. https://doi.org/10.1038/srep25520

488 Rutkowska, Aleksandra, O'Sullivan, S.A.S.A.S.A., Christen, I., Zhang, J., Sailer, A.W.A.W., Dev,
489 K.K.K.K., 2016. The EBI2 signalling pathway plays a role in cellular crosstalk between
490 astrocytes and macrophages. Sci. Rep. 6, 25520. https://doi.org/10.1038/srep25520

491 Rutkowska, A., Preuss, I., Gessier, F., Sailer, A.W.A.W., Dev, K.K.K.K., 2015. EBI2 regulates
492 intracellular signaling and migration in human astrocyte. Glia 63, 341–351.
493 https://doi.org/10.1002/glia.22757

494 Rutkowska, A., Sailer, A.W., Dev, K.K., 2017. EBI2 receptor regulates myelin development and
495 inhibits LPC-induced demyelination. J. Neuroinflammation 14, 250.
496 https://doi.org/10.1186/s12974-017-1025-0

497 Rutkowska, A., Shimshek, D.R., Sailer, A.W., Dev, K.K., 2018. EBI2 regulates pro-inflammatory
498 signalling and cytokine release in astrocytes. Neuropharmacology 133, 121–128.
499 https://doi.org/10.1016/j.neuropharm.2018.01.029

500 Spencer, J.I., Bell, J.S., DeLuca, G.C., 2018. Vascular pathology in multiple sclerosis: reframing
501 pathogenesis around the blood-brain barrier. J. Neurol. Neurosurg. Psychiatry 89, 42–52.
502 https://doi.org/10.1136/jnnp-2017-316011

503 Tang, J., Shi, Y., Zhan, L., Qin, C., 2020. Downregulation of GPR183 on infection restricts the early

504 infection and intracellular replication of mycobacterium tuberculosis in macrophage. Microb.
505 Pathog. 145. https://doi.org/10.1016/j.micpath.2020.104234

506 Velasco-Estevez, M., Koch, N., Klejbor, I., Laurent, S., Dev, K.K., Szutowicz, A., Sailer, A.W.,
507 Rutkowska, A., 2021. Ebi2 is temporarily upregulated in mo3.13 oligodendrocytes during
508 maturation and regulates remyelination in the organotypic cerebellar slice model. Int. J. Mol. Sci.
509 22. https://doi.org/10.3390/ijms22094342

510 Wang, P., You, S.W., Yang, Y.J., Wei, X.Y., Wang, Y.Z., Wang, X., Hao, D.J., Kuang, F., Shang,
511 L.X., 2014. Systemic Injection of Low-Dose Lipopolysaccharide Fails to Break down the Blood–
512 Brain Barrier or Activate the TLR4-MyD88 Pathway in Neonatal Rat Brain. Int. J. Mol. Sci.
513 2014, Vol. 15, Pages 10101-10115 15, 10101–10115. https://doi.org/10.3390/IJMS150610101

514 Wanke, F., Moos, S., Croxford, A.L., Heinen, A.P., Gräf, S., Kalt, B., Tischner, D., Zhang, J.,
515 Christen, I., Bruttger, J., Yogev, N., Tang, Y., Zayoud, M., Israel, N., Karram, K., Reißig, S.,
516 Lacher, S.M., Reichhold, C., Mufazalov, I.A., Ben-Nun, A., Kuhlmann, T., Wettschureck, N.,
517 Sailer, A.W., Rajewsky, K., Casola, S., Waisman, A., Kurschus, F.C., 2017. EBI2 Is Highly
518 Expressed in Multiple Sclerosis Lesions and Promotes Early CNS Migration of Encephalitogenic
519 CD4 T Cells. Cell Rep. 18, 1270–1284. https://doi.org/10.1016/j.celrep.2017.01.020

520 Yi, T., Wang, X., Kelly, L.M.M., An, J., Xu, Y., Sailer, A.W.W., Gustafsson, J.-A.A., Russell,
521 D.W.W., Cyster, J.G.G., 2012. Oxysterol Gradient Generation by Lymphoid Stromal Cells
522 Guides Activated B Cell Movement during Humoral Responses. Immunity 37, 535–548.
523 https://doi.org/10.1016/j.immuni.2012.06.015

524

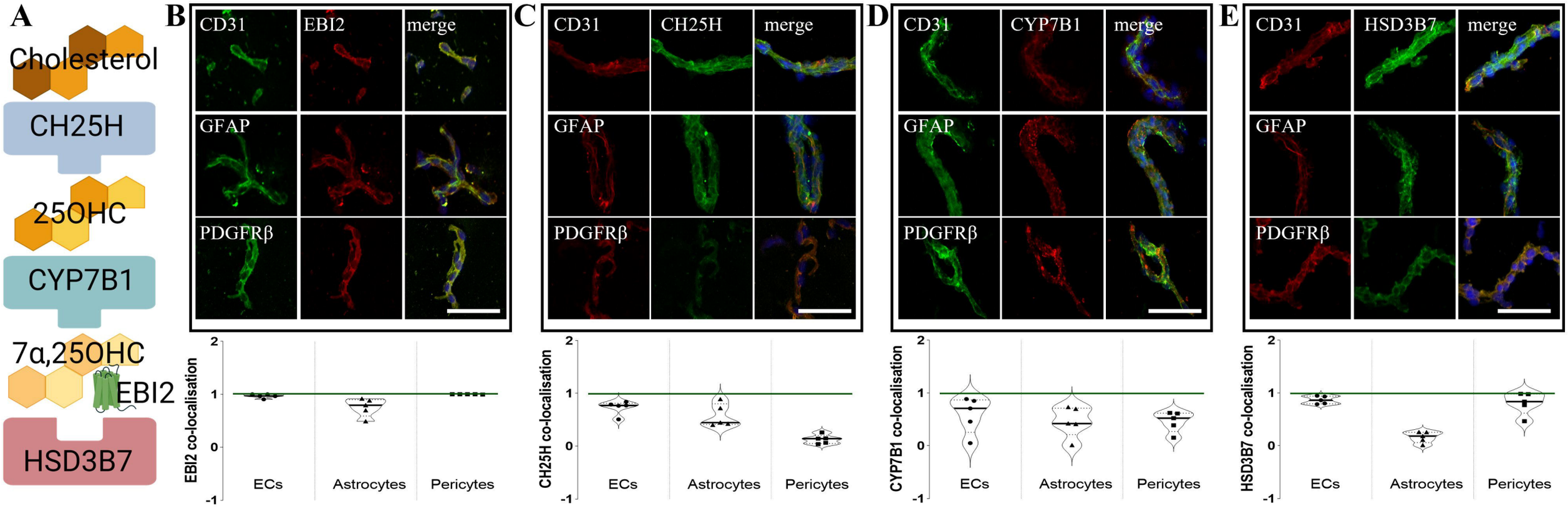

Figure 1. The oxysterol 7α,25OHC synthesising (CH25H, CYP7B1) and degrading (HSD3B7) enzymes are present in the mouse brain microvascular cells. A. Schematic representation of the synthetic and degrading pathway of 7α,25OHC, the endogenous ligand for EBI2. **B.** EBI2 was detected in the isolated brain microvessels. The highest co-colocalisation was detected with the pericyte (PDGFRβ+ 0.99 +/- 0.003) and EC (CD31+ 0.97 +/-0.09) markers. **C.** The first enzyme in the 7α,25OHC synthetic pathway, CH25H, was detected in CD31+ (ECs), GFAP+ (astrocytic endfeet) and PDGFRβ+ (pericytes/smooth muscle cells) cells with the highest co-localisation with the EC marker CD31 (0.73 range 0.33) and lowest with the pericyte marker PDGFRβ (0.13 +/- 0.22). **D.** The second enzyme, CYP7B1, moderately co-localised with all three cell markers, CD31 (0.59 +/-0.83), GFAP (0.45 +/-0.72) and PDGFRβ (0.46 +/-0.47). **E.** The 7α,25OHC degrading enzyme, HSD3B7 mostly co-localised with the EC+ (0.87 +/-0.16) and pericyte/smooth muscle cells (0.81 +/-0.52) cells and least with astrocytes (0.16 +/-0.52). Scale 50 µm. Data shown as violin plot with median (solid line) and quartiles (dotted line); 1=complete co-localisation (solid line) and 0=no co-localisation, N= microvessels isolated from 8 mouse brains.

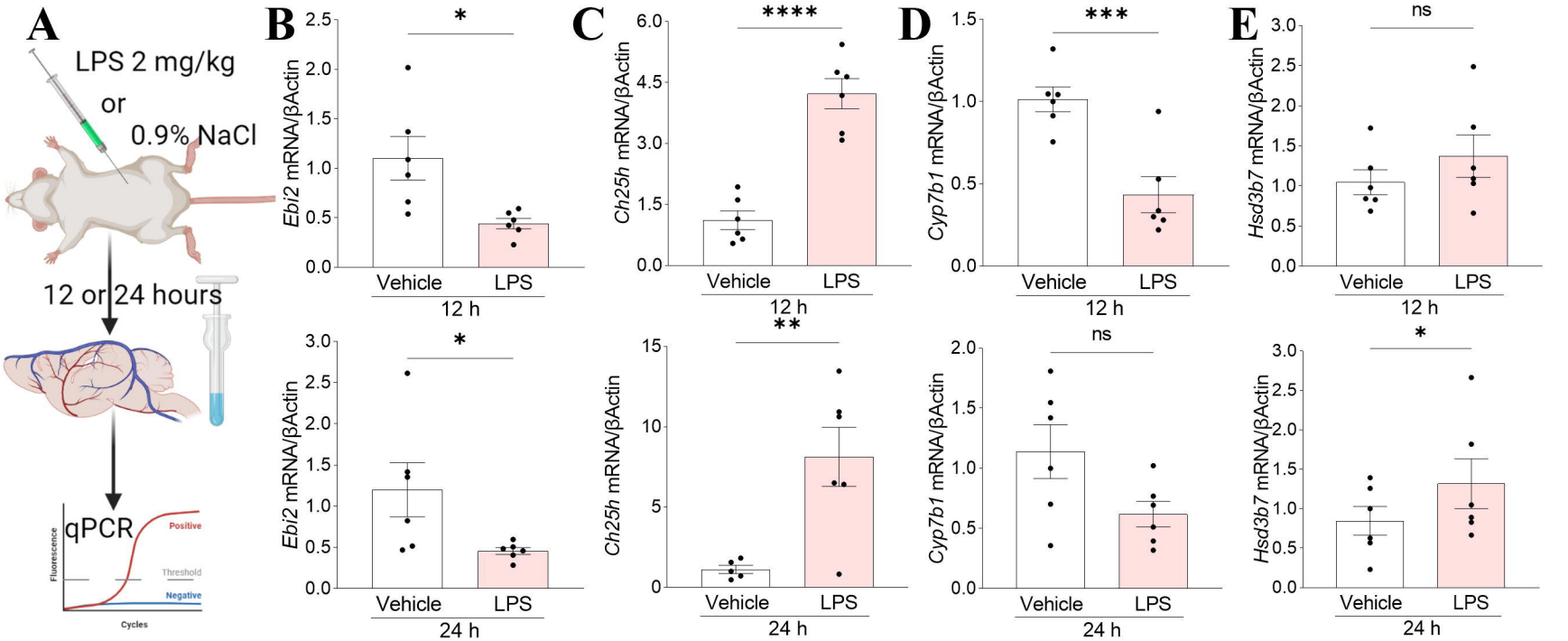

Figure 2. Systemic inflammation induces changes in the expression of Ebi2 and Ch25H, Cyp7b1 and Hsd3b7 enzymes in the mouse brain. A. Schematic representation of experimental setup. **B.** The expression of *Ebi2* in whole brain homogenates decreased after 12 and 24 hours of LPS treatment (12 h: 40% +/- 2% vs. vehicle; 24 h: 38% +/- 4% vs. vehicle). **C.** The mRNA expression of the *Ch25h* enzyme in the mouse brain increased after 12 and 24 hours post LPS injection (12 h: 382% +/- 34% vs. vehicle; 24 h: 725% +/- 164% vs. vehicle). **D.** The mRNA levels of the *Cyp7b1* enzyme decreased 12 hours after LPS treatment (43% +/- 11% vs. vehicle). **E.** The 7α,25OHC degrading enzyme, *Hsd3b7*, increased after 24 hours of LPS treatment (153% +/- 38% vs. vehicle). Data presented as mean + /− SEM, n=6 mice, unpaired student t-tests, *p<0.05, **p<0.01, ***p<0.001, ****p<0.0001 vs. corresponding vehicle.

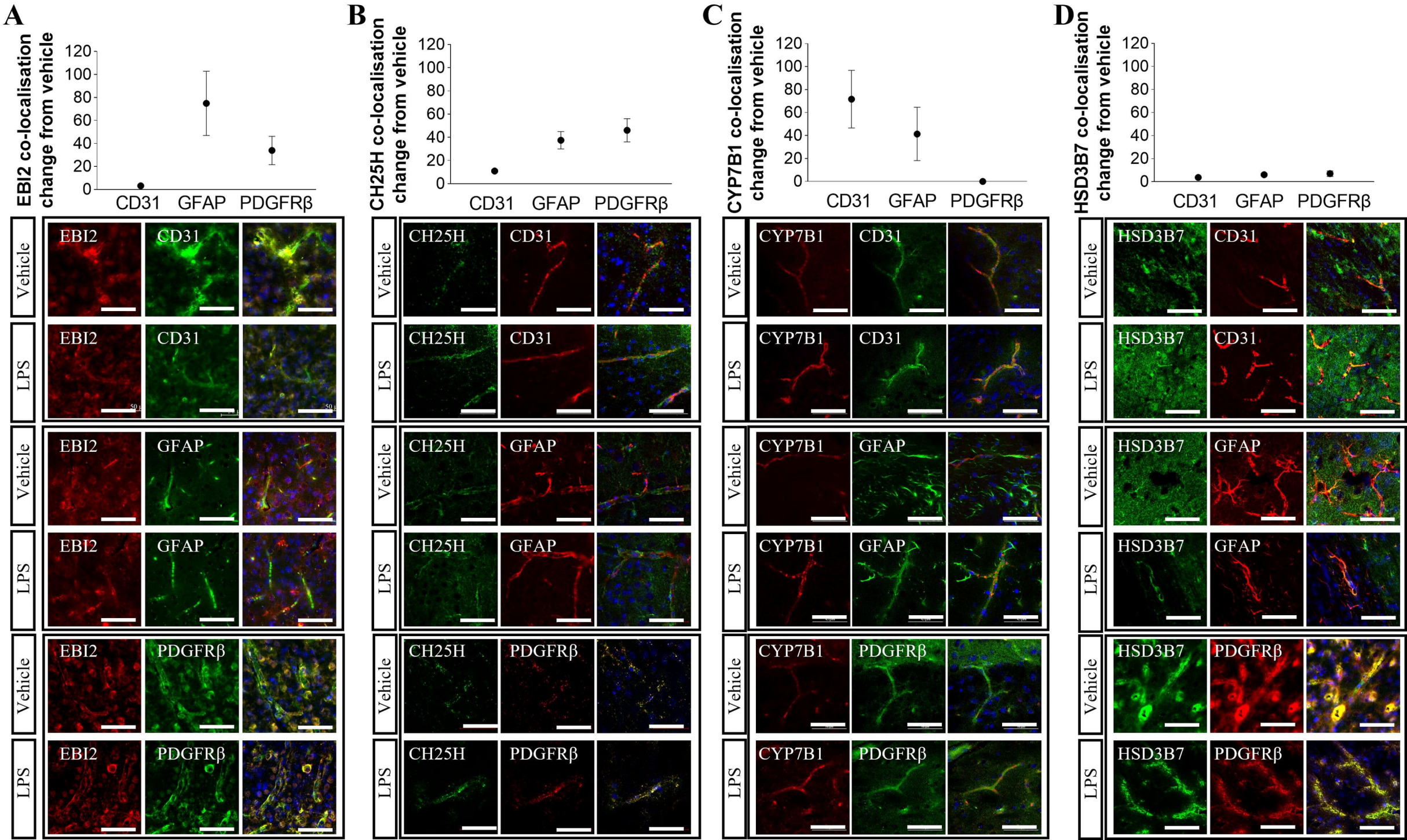
A
EBI2 co-localisation change from vehicle
120
100
80
60
40
20
0
CD31
GFAP
PDGFRβ
B
CH25H co-localisation change from vehicle
C
CYP7B1 co-localisation change from vehicle
D
HSD3B7 co-localisation change from vehicle
Vehicle
LPS
EBI2
CD31
GFAP
PDGFRβ
CH25H
CYP7B1
HSD3B7

Figure 3. Systemic inflammation induces 7α,25OHC synthesising enzymes in the mouse brain vascular cells. A. The density of EBI2 in CD31+ cells did not increased after LPS treatment. The biggest increase in EBI2 was observed in GFAP+ cells (75% +/-28%) and a moderate increase in PDGFRβ+ cells (34% +/-12%). **B.** The density of the first enzyme in the 7α,25OHC synthetic pathway, CH25H, increased after LPS by 46% (+/-10) in PDGFRβ+ cells and 38% (+/-7.4%) in GFAP+ cells. The density in CD31+ (ECs) remained most stable with an increase of 11% (+/-1%) after LPs challenge. **C.** In contrast, the density of the second synthesising enzyme, CYP7B1, increased mostly in CD31+ cells (72% +/-25%), followed by GFAP+ cells (41% +/-23%) and no change in PDGFRβ+ cells. **D.** The 7α,25OHC degrading enzyme, HSD3B7, was the least affected by systemic inflammation with density increasing in CD31+ cells by 3.8% (+/-0.56%), 7% (+/-2.4%) in PDGFRβ+ cells and 6.2% (+/-1.2%) in GFAP+ cells. Data presented as mean +/- SEM (N=6 mice) after normalisation to vehicle (=1). Immunostaining of blood vessels in the cortex was performed on brain sections cut in the coronal plane (sections corresponding to levels 70-87 in Allen Mouse Brain Atlas).